J. Phys. Chem. A **2002,** *106,* 8201−8206

A Comparative ab Initio Multireference Single and Double Excitation Configuration Interaction Study of the Electronic Spectra of Low-Lying Linear and Cyclic C_5H Isomers

Jan Haubrich, Max Mühlhäuser,* and Sigrid D. Peyerimhoff

Institut fur Physikalische und Theoretische Chemie der Universität Bonn, Wegelerstrasse 12, 53115 Bonn, Germany

Received: June 6, 2002; In Final Form: July 18, 2002

Multireference configuration interaction (MRD-CI) calculations are performed to compute the electronic spectra of the three low-lying isomers of C_5H, a molecule of radio-astronomical interest. The electronic spectrum of linear C_5H is dominated by two transitions computed at 4.13 eV ($^2\Pi \leftarrow X^2\Pi$) and 6.11 eV ($^2\Pi \leftarrow X^2\Pi$). The first dipole-allowed transition is calculated at 2.54 eV ($^2\Delta \leftarrow X^2\Pi$). Further relatively strong excitations are obtained at 2.71 eV ($^2\Sigma^- \leftarrow X^2\Pi$) and 4.00 eV ($^2\Pi \leftarrow X^2\Pi$). The first dipole-allowed excitation of a C_{2v} symmetric ring-chain isomer is calculated at 1.27 eV ($^2A_1 \leftarrow X^2B_2$). Up to 3.61 eV ($^2A_2 \leftarrow X^2B_2$), no other dipole-allowed transitions are obtained, whereas the spectrum of a C_s symmetric ring-chain structure shows several dipole-allowed excitations in the energy interval between 0.85 and 2.53 eV, including a dominating transition computed at 1.67 eV ($^2A' \leftarrow X^2A'$).

1. Introduction

Besides pure carbon clusters, C_n ($n < 20$), and their cationic and anionic forms, small hydrocarbon clusters have attracted considerable theoretical and experimental interest during recent years.[1−22] These hydrocarbon clusters are discussed as possible carriers of the diffuse interstellar bands (DIBs)[11,14,15,22] and are most likely precursors of larger carbon clusters of scientific interest for fullerene formation.

Linear C_5H has been identified by Gottlieb et al.[18] in 1986 employing microwave spectroscopy. In the same year, Cernicharo et al.[19] reported the astrochemical identification of linear C_5H. Further mass-spectrometric and theoretical studies of C_5H and its anions were performed by Blanksby et al.,[20] who identified a branched C_2-CH-C_2 isomer lying relatively high in energy. Recently, Crawford et al.[21] calculated the structure and energetics of possible low-lying C_5H isomers using coupled cluster methods. Although considerable effort has been made to identify cyclic isomers of C_5H, which are predicted to be low-lying by recent calculations,[21] cyclic C_5H is not yet experimentally identified. Thus the goal of the present work is to employ theoretical methods to further characterize certain properties of these molecules to help experimental search.

To differentiate between the linear and the two low-lying cyclic isomers of C_5H, one possible approach is employing spectroscopic techniques to search for characteristic fingerprints in the electronic absorption spectrum. Although real fingerprints include not only band approximate position and relative intensity but also its shape determined by the vibrational structure, theoretical studies are an almost ideal tool to provide a firm foundation upon which experimentalists can design strategies for interrogating these short-lived species with greater confidence. Such work has recently been successful for a number of carbon clusters,[4−10] and with the present study, we extend our work to C_5H.

2. Computational Techniques

The equilibrium geometries of the linear and the two cyclic isomers of C_5H are adopted from ref 21. They were obtained employing coupled cluster calculations. For completeness, they are given in Figure 1.

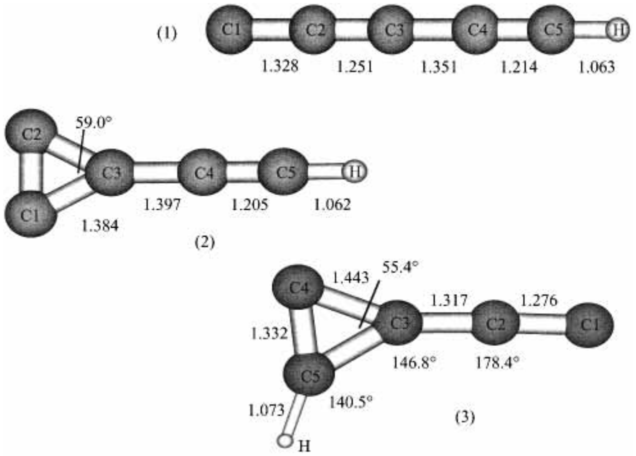

Figure 1. Equilibrium geometries of the linear isomer **1** of C_5H and cyclic ring-chain isomers **2** and **3**. The values given are adopted from ref 21.

The computations of the electronically excited states were performed with the multireference single and double excitation configuration interaction method (MRD-CI) implemented in the DIESEL program.[23] The automatic selection of reference configurations was carried out with a summation threshold of 0.85 for the linear isomer and 0.82 for both cyclic isomers, which means that the sum of the squared coefficients of all reference configurations selected for each state (root) is above this threshold. The set of reference configurations per irreducible representation (IRREP) was in the range between 22 and 50 for the linear isomer. On the basis of the summation threshold of 0.82, between 7 and 10 reference configurations per IRREP were selected for the cyclic isomer **2** and between 7 and 13 reference configurations per IRREP for cyclic isomer **3**. An analysis of the molecular orbitals (MO) occupied in these reference configurations justified the prior choice of treating 21 electrons active in all three molecules, while keeping the remaining electrons in doubly occupied orbitals (frozen).

---

* To whom correspondence should be addressed. Fax: +49-0228-739064. E-mail: max@thch.uni-bonn.de.

10.1021/jp021374c CCC: $22.00 © 2002 American Chemical Society
Published on Web 08/10/2002

From the set of reference configurations (mains), all single and double excitations in the form of configuration state functions (CSFs) are generated and all configurations with an energy contribution $\Delta E(T)$ above a given threshold T are selected, that is, the contribution of a configuration larger than this value relative to the energy of the reference set is included in the final wave function.

A selection threshold of $T = 1 \times 10^{-7}$ hartree was used for the linear and for both cyclic isomers of C_5H. The effect of those configurations that contribute less than T is accounted for in the energy computation (E(MRD-CI)) by a perturbative technique.[24] The contribution of higher excitations is estimated by applying a generalized Langhoff−Davidson correction formula $E(\text{MRD-CI+Q}) = E(\text{MRD-CI}) - (1 - c_0^2)[E(\text{ref}) - E(\text{MRD-CI})]/c_0^2$, where c_0^2 is the sum of squared coefficients of the reference species in the total CI wave function and E(ref) is the energy of the reference configurations. The MRD-CI calculations of the linear form are performed in the abelian subgroup C_{2v}. Therefore states of Σ^+ and Δ, as well as Σ^- and Δ, are computed in the same IRREP. Furthermore Π and Φ states are found in the same IRREP. To keep the computation at a manageable size, only up to a maximum of six doublet states per IRREP are computed for both cyclic isomers. For the linear isomer, six doublet states in IRREPs of Σ, Δ, and Γ symmetry and eight roots in IRREPs of Π and Φ symmetry are computed.

The number of selected configuration state functions directly included in the energy calculations are as large as 1.6 million (linear), 2.8 million (isomer **2**), and 5.8 million (isomer **3**) selected from a total space of 19.2 million (linear), 4 million (isomer **2**), and 7.9 million (isomer **3**) generated configurations.

For our calculations for hydrogen, we used a correlation consistent AO basis set of double-ζ quality (cc-pVDZ),[26] and for carbon, we employed an AO basis set taken from Huzinage−Dunning[25] that consists of 9s5p Gaussians in a 5s3p contraction and an additional d polarization function with an exponent of $\alpha = 0.75$. Previous work on the carbon clusters C_n ($n = 5$, 6)[5,9] showed that enlarging this basis by Rydberg functions or by employing more functions in the polarization and correlation description will change the results for transition energies generally by less than 0.25 eV. This basis is flexible with respect to polarization and electron correlation and is considered to be fairly balanced for all states treated.

In addition, we computed five doublet states per IRREP of the linear isomer (**1**) also using a larger basis set of triple-ζ quality (cc-pVTZ)[26] augmented by two s and one p Rydberg functions at the carbon center C(3) (Figure 1). The exponents taken are $\alpha_{s1} = 0.03$, $\alpha_{s2} = 0.015$, and $\alpha_p = 0.02$. As expected, the changes between cc-pVDZ and cc-pVTZ+SSP results are generally less than 0.25 eV (Table 2). The calculated oscillator strengths are also in general agreement. These results support our long-time experience that CI calculations employing the more economic double-ζ basis set[25] give realistic results for molecular excited states.

3. Results and Discussion

The C_5H cluster is known to possess three low-lying isomers: a $C_{\infty v}$ symmetric linear chain isomer ($X^2\Pi$ state), a cyclic ring-chain structure with C_{2v} symmetry (X^2B_2 ground state), and a cyclic ring-chain form with C_s symmetry (X^2A').[21] The equilibrium geometries are given in Figure 1, and MO schemes of these isomers are illustrated in Figures 2−4.

For the relative stability of cyclic isomer **2** of C_5H against the linear isomer **1**, we obtain ΔE(MRD-CI+Q) = 6.0 kcal/mol in favor of the linear structure. This value is in reasonable agreement with both the 5.5 kcal/mol obtained by Crawford et al. at the CCSD level and his CCSD(T) single-point estimation of 6.3 kcal/mol.[21] We computed isomer **3** ΔE(MRD-CI+Q) = 22.6 kcal/mol above the linear form. Crawford et al. calculated isomer **3** to be 26.4 kcal/mol higher in energy than the linear form at CCSD level and 23.9 kcal/mol higher when using CCSD(T) single-point methods,[21] so our results show reasonable agreement with the values obtained by Crawford et al. for isomer **3**, too.

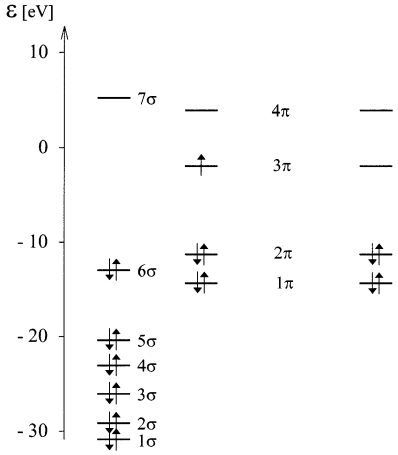

Figure 2. Schematic diagram of the MO energy spectrum of the ground-state configuration of linear C_5H. The values were obtained at the SCF level. Occupied MOs are marked with arrows.

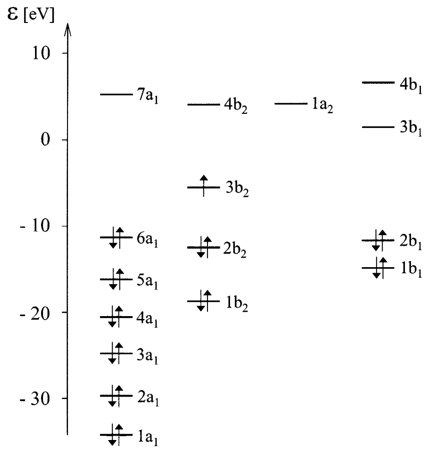

Figure 3. Schematic diagram of the MO energy spectrum of the ground-state configuration of C_5H isomer **2** (Figure 1). The values were obtained at the SCF level, and occupied MOs are marked with arrows.

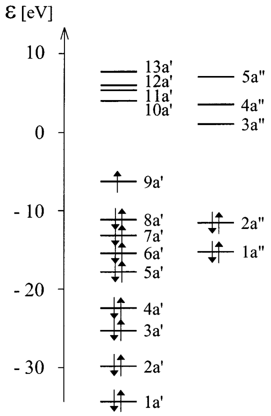

Figure 4. Schematic diagram of the MO energy spectrum of the ground-state configuration of C_5H isomer **3** (Figure 1). The values were obtained at the SCF level. Occupied MOs are marked with arrows.

TABLE 1: Low-Lying Doublet Electronic States of the Linear C_5H as Expected from Qualitative MO Theory[a]

excitation	configuration	states
	$3\pi^1$	$X^2\Pi$
$6\sigma \rightarrow 3\pi$	$6\sigma^1\ 2\pi^4\ 3\pi^2$	$^2\Sigma^+$, $^2\Sigma^-$, $^2\Delta$
$2\pi \rightarrow 3\pi$	$2\pi^3\ 3\pi^2$	$^2\Pi(3)$, $^2\Phi$
$3\pi \rightarrow 4\pi$	$4\pi^1$	$^2\Pi$
$6\sigma \rightarrow 4\pi$	$6\sigma^1\ 2\pi^4\ 3\pi^1\ 4\pi^1$	$^2\Sigma^+(2)$, $^2\Sigma^-(2)$, $^2\Delta(2)$
$1\pi \rightarrow 3\pi$	$1\pi^3\ 6\sigma^2\ 2\pi^4\ 3\pi^2$	$^2\Pi(3)$, $^2\Phi$
$5\sigma \rightarrow 3\pi$	$5\sigma^1\ 1\pi^4\ 6\sigma^2\ 2\pi^4\ 3\pi^2$	$^2\Sigma^+$, $^2\Sigma^-$, $^2\Delta$
$2\pi \rightarrow 4\pi$	$2\pi^3\ 3\pi^1\ 4\pi^1$	$^2\Pi(6)$, $^2\Phi(2)$
$6\sigma\ 2\pi \rightarrow 3\pi^2$	$6\sigma^1\ 2\pi^3\ 3\pi^3$	$^2\Sigma^+(2)$, $^2\Sigma^-(2)$, $^2\Delta(2)$
$2\pi\ 3\pi \rightarrow 4\pi^2$	$6\sigma^2\ 2\pi^3\ 3\pi^0\ 4\pi^2$	$^2\Pi(3)$, $^2\Phi$
$6\sigma\ 3\pi \rightarrow 4\pi^2$	$6\sigma^1\ 2\pi^4\ 3\pi^0\ 4\pi^2$	$^2\Sigma^+$, $^2\Sigma^-$, $^2\Delta$

[a] The ground-state $X^2\Pi$ state configuration is ...$5\sigma^2\ 1\pi^4\ 2\pi^4\ 6\sigma^2\ 3\pi^1/7\sigma^0\ 4\pi^0$ (valence electrons only).

TABLE 2: Calculated Transition Energies, ΔE (eV), and Oscillator Strengths, f, from the $X^2\Pi$ State of Linear C_5H to Its Low-Lying Electronic States[a]

state	excitation	ΔE^b	f^b	ΔE^c	f^c
$X^2\Pi$	ground state	0.0		0.0	
$^2\Delta$	$6\sigma \rightarrow 3\pi$	2.54	0.003	2.62	0.003
$^2\Sigma^-$	$6\sigma \rightarrow 3\pi$	2.71	0.009	2.80	0.007
$^2\Sigma^+$	$6\sigma \rightarrow 3\pi$	3.09	0.005	3.19	0.009
$^2\Pi$	$2\pi \rightarrow 3\pi$	3.11	0.001	3.21	0.001
$^2\Phi$	$2\pi \rightarrow 3\pi$	3.73	0	3.60	0
$^2\Pi$	$2\pi \rightarrow 3\pi$ $3\pi \rightarrow 4\pi$	4.00	0.007	3.99	0.004
$^2\Pi$	$3\pi \rightarrow 4\pi$ $2\pi \rightarrow 3\pi$	4.13	0.03	4.19	0.03
$^2\Sigma^-$	$6\sigma\ 2\pi \rightarrow 3\pi^2$ $(6\sigma \rightarrow 4\pi)$	5.00	0.001	5.25	0.001
$^2\Pi$	$1\pi \rightarrow 3\pi$	5.10	0.005		
$^2\Phi$	$1\pi \rightarrow 3\pi$	5.48	0		
$^2\Delta$	$6\sigma\ 2\pi \rightarrow 3\pi^2$ $(6\sigma \rightarrow 4\pi)$	5.91	0.001	5.92	0.001
$^2\Pi$	$1\pi \rightarrow 3\pi$	6.11	0.14		
$^2\Delta$	$6\sigma\ 2\pi \rightarrow 3\pi^2$ $(6\sigma \rightarrow 4\pi)$	6.14	0.002	6.05	0.002
$^2\Sigma^-$	$6\sigma\ 2\pi \rightarrow 3\pi^2$ $(6\sigma \rightarrow 4\pi)$	6.22	0.001		
$^2\Sigma^+$	$6\sigma\ 2\pi \rightarrow 3\pi^2$ $(6\sigma \rightarrow 4\pi)$	6.28	0.001		
$^2\Pi$	$1\pi \rightarrow 3\pi$	6.35	0.001		
$^2\Sigma^+$	$6\sigma\ 2\pi \rightarrow 3\pi^2$ $(6\sigma \rightarrow 4\pi)$	7.01	0.002		

[a] The electronic configuration of the $X^2\Pi$ state is ...$5\sigma^2\ 1\pi^4\ 2\pi^4\ 6\sigma^2\ 3\pi^1/7\sigma^0\ 4\pi^0$. The f values are only for one component of the degenerate state in the abelian subgroups. For comparison, the results obtained with the use of a cc-p-VTZ+SSP basis sets, as discussed in the text, are also included. [b] Basis set of Huzinage−Dunning[25,26] with double-ζ quality. [c] cc-p-VTZ+SP basis set[26] of triple-ζ quality.

3.1. Linear C_5H. The ground-state configuration of linear C_5H is ... $5\sigma^2\ 1\pi^4\ 2\pi^4\ 6\sigma^2\ 3\pi^1/7\sigma^0\ 4\pi^0$. Possible low-energy doublet states relative to this configuration are listed in Table 1. Because the energy levels of 1π, 6σ, and 2π are fairly close (Figure 2), single excitations from all three fully occupied valence molecular orbitals (MOs) into the singly occupied 3π are expected to lead to low-energy states. For the same reason, excitations into the 4π LUMO involving a combination of 1π, 6σ, 2π, and 3π are likely to occur.

The vertical excitation energies obtained for the first electronically excited states are listed in Table 2, together with the corresponding oscillator strengths, f. As can be seen from Table 2 in conjunction with Table 1, the lowest dipole-allowed transition, $^2\Delta \leftarrow X^2\Pi$, computed at 2.54 eV corresponds to $6\sigma \rightarrow 3\pi$ excitation. This excitation gives also rise to the $^2\Sigma^-$ at 2.71 eV and $^2\Sigma^+$ states calculated at 3.09 eV. All states resulting from this excitation show oscillator strengths f of similar magnitude.

TABLE 3: Calculated Transition Energies, ΔE (eV), and Oscillator Strengths, f, from the X^2B_2 Ground State of the Cyclic Isomer 2 of C_5H to Excited Electronic States[a]

state	excitation	ΔE	f
$X1^2B_2$	ground state	0.0	
1^2A_1	$6a_1 \rightarrow 3b_2$	1.27	0.02
1^2B_1	$3b_2 \rightarrow 3b_1$	3.15	0
1^2A_2	$3b_2 \rightarrow 1a_2$	3.61	0.0008
2^2B_1	$2b_1 \rightarrow 3b_2$	4.05	0
2^2B_2	$2b_2 \rightarrow 3b_2$	4.09	0.01
2^2A_2	$6a_1 \rightarrow 3b_1$ $6a_1\ 2b_2 \rightarrow 3b_2\ 3b_1$	4.48	0.02
3^2A_2	$6a_1\ 2b_2 \rightarrow 3b_2\ 3b_1$ $6a_1 \rightarrow 3b_1$	5.05	0.004
3^2B_2	$2b_1 \rightarrow 3b_1$	5.23	0.005
2^2A_1	$5a_1 \rightarrow 3b_2$	5.65	0.02
4^2B_2	$3b_2 \rightarrow 4b_2$	5.97	0.003
3^2B_1	$1b_1 \rightarrow 3b_2$	5.98	0
4^2B_1	$6a_1 \rightarrow 1a_2$ $3b_2 \rightarrow 4b_1$	6.07	0
5^2B_1	$2b_2 \rightarrow 3b_1$	6.28	0
3^2A_1	$6a_1\ 2b_1 \rightarrow 3b_2\ 3b_1$	6.29	0.002
6^2B_1	$3b_2 \rightarrow 4b_1$ $6a_1 \rightarrow 1a_2$	6.59	0
5^2B_2	$1b_2 \rightarrow 3b_2$	7.04	0.06
4^2A_1	$6a_1 \rightarrow 4b_2$ $6a_1\ 2b_2 \rightarrow 3b_2\ 4b_2$	7.08	0.01
4^2A_2	$6a_1\ 2b_2 \rightarrow 3b_2\ 3b_1$ $6a_1\ 2b_1 \rightarrow 3b_1^2$	7.12	0.0002
5^2A_2	$6a_1\ 2b_1 \rightarrow 3b_1^2$ $6a_1\ 2b_2 \rightarrow 3b_2\ 3b_1$	7.20	0.0001
5^2A_1	$6a_1\ 2b_2 \rightarrow 3b_2\ 4b_2$ $6a_1 \rightarrow 4b_2$	7.41	0.0003

[a] The X^2B_2 ground-state configuration is ...$5a_1^2\ 1b_1^2\ 2b_2^2\ 2b_1^2\ 6a_1^2\ 3b_2^1/3b_1^0\ 4b_2^0\ 7a_1^0$ (valence electrons only).

The excitation $2\pi \rightarrow 3\pi$ results in the two $^2\Pi$ states obtained at 3.11 and 4.00 eV and a $^2\Phi$ state computed at 3.73 eV. The latter $^2\Pi$ state shows multireference character because of a contribution from the $3\pi \rightarrow 4\pi$ excitation, which is similar in energy to the $2\pi \rightarrow 3\pi$ transition. The corresponding state to this linear combination is computed at 4.13 eV and is obtained like the $^2\Pi$ state at 4.00 eV with considerable oscillator strength. Because the excitation $3\pi \rightarrow 4\pi$ is of $\pi-\pi^*$ type for C(1)C(2) and C(3)C(4), the larger intensity can be expected. The excitation $1\pi \rightarrow 3\pi$ is also $\pi-\pi^*$ type and gives rise to three $^2\Pi$ states and a $^2\Phi$ state calculated at 5.10, 6.11, 6.35, and 5.48 eV.

The double excitation $6\sigma\ 2\pi \rightarrow 3\pi^2$ leads to two $^2\Sigma^-$ states computed at 5.00 and 6.22 eV, two $^2\Delta$ states at 5.91 and 6.14 eV, and two $^2\Sigma^+$ states obtained at 6.28 and 7.01 eV. The analysis of reference configurations shows for all of these states some contribution of $6\sigma \rightarrow 4\pi$ excitation.

The transition energies employing the larger AO basis set are seen to be generally increased, and closer analysis shows that it is the ground-state energy that is preferentially lowered (by 0.005−0.008 hartree) relative to the energy of the excited states. It is not clear, however, whether the excitation energies in the more flexible AO basis are more realistic because the larger basis leads also to a larger space of virtual orbitals and consequently to a slower convergence of the CI expansion. The differences can be taken as approximate error bars for the calculated data, however.

3.2. Cyclic C_5H Isomer 2. In Table 3, the results that we obtained for the cyclic isomer **2** of C_5H are summarized. The orbital energy diagram of its ground state is given in Figure 3. Charge density contours of characteristic valence and low-lying virtual orbitals of C_5H isomer **2** are presented in Figure 5. The doublet X^2B_2 ground state of this ring-chain isomer **2** possesses

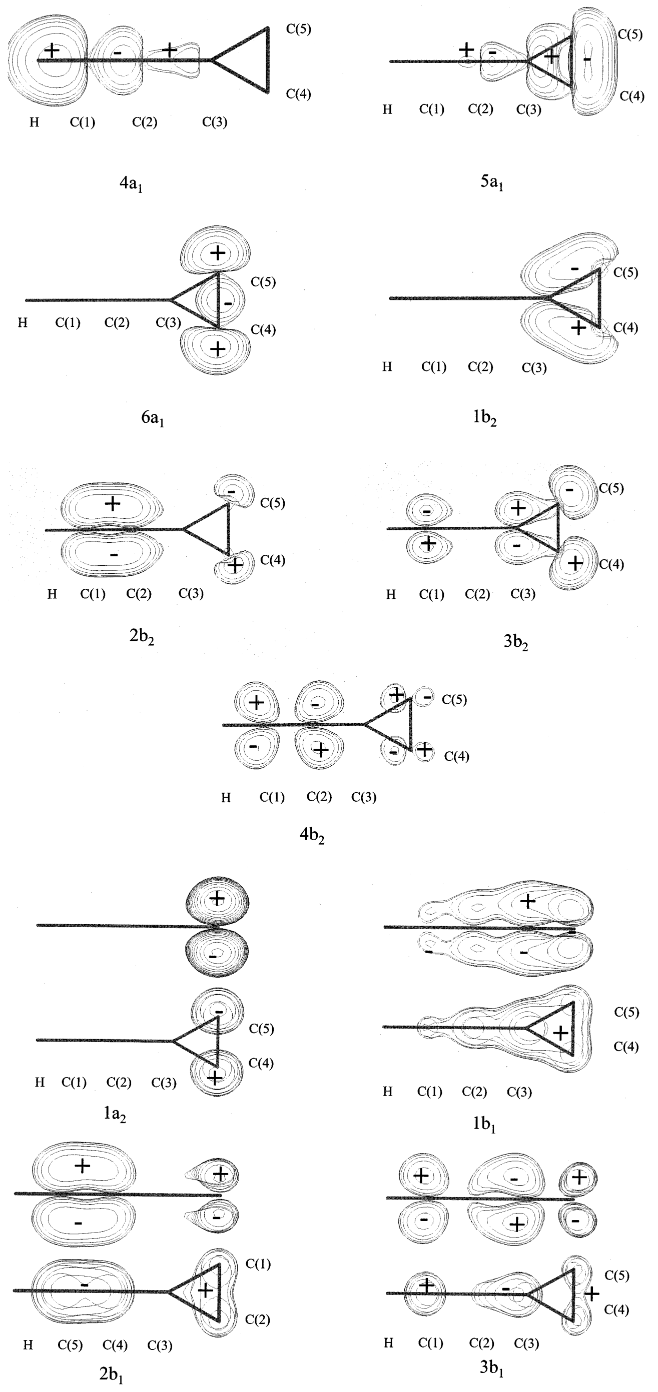

Figure 5. Charge density contours (contour value of 0.07) of characteristic valence and low-lying virtual (1a$_2$, 4b$_2$, 3b$_1$) orbitals of the cyclic isomer **2** (Figure 1). The energetic ordering can be seen from Figure 3. For the out-of-plain orbitals of a$_2$ and b$_1$ symmetry, contour lines are given in two orthogonal planes.

the electron configuration ...5a$_1^2$ 1b$_1^2$ 2b$_2^2$ 2b$_1^2$ 6a$_1^2$ 3b$_2^1$. The occupied molecular orbitals (MOs) 6a$_1$, 2b$_1$, 2b$_2$, and to a lesser extent 5a$_1$, 1b$_1$, and 1b$_2$ are close in energy and also close to the singly occupied 3b$_2$ orbital (SOMO). Furthermore, the energy differences of 3b$_2$ (SOMO) to the virtual orbitals 3b$_1$, 1a$_2$, 4b$_2$, 4b$_1$, and 7a$_1$ are also similar. Therefore, low-energy transitions between these levels can be expected.

As expected on the basis of the qualitative picture (Figure 3), the lowest state results from a 6a$_1$ → 3b$_2$ excitation, calculated at 1.27 eV. Excitations from 2b$_1$ and 2b$_2$ into 3b$_2$ are obtained close in energy, while excitations from the lower-lying MOs 5a$_1$, 1b$_1$, and 1b$_2$ into the SOMO 3b$_2$ are computed at higher energies (5.5−7 eV). All transitions (with the exception of the b$_1$ → b$_2$ excitations forbidden by the dipole selection rules) show relatively high intensity. The highest intensity is calculated for the 1b$_2$ → 3b$_2$ transition. All other allowed transitions into 3b$_2$ show about the same *f* value, which can be rationalized because the lower orbital shows always orthogonal nodal planes relative to the upper 3b$_2$ orbital but its charge is concentrated in the same spatial area. The *f* value of 0.06 can be understood because the character of the 1b$_2$ MO is in-plane bonding at C(3)C(4) and C(3)C(5), whereas 3b$_2$ is antibonding for these centers. Thus, the resulting excitation is of (in-plane) $\pi-\pi^*$[C(3)C(4), C(3)C(5)]-type, for which considerable oscillator strength can be expected.

TABLE 4: Calculated Transition Energies, Δ*E* (eV), and Oscillator Strengths, *f*, from the X^{2}A′ Ground State of the Cyclic Isomer 3 of C$_5$H to Excited Electronic States[a]

state	excitation	Δ*E*	*f*
X1^{2}A′	ground state	0.0	
2^{2}A′	8a′ → 9a′ 7a′ → 9a′	0.85	0.001
3^{2}A′	7a′ → 9a′ 8a′ → 9a′	1.67	0.06
1^{2}A″	2a″ → 9a′	1.93	0.0003
2^{2}A″	9a′ → 3a″	2.53	0.0007
3^{2}A″	7a′ 8a′ → 9a′ 3a″ 8a′ → 3a″	3.10	0.0006
4^{2}A″	8a′ → 3a″ 7a′ 8a′ → 9a′ 3a″	3.83	0.02
4^{2}A′	2a″ → 3a″	3.89	0.0007
5^{2}A″	9a′ → 4a″	3.93	0.0006
6^{2}A″	7a′ → 3a″	3.98	0.0003
5^{2}A′	6a′ → 9a′	4.59	0.03
6^{2}A′	9a′ → 10a′	4.87	0.02

[a] The X^{2}A′ ground-state configuration is ...(5a′)^2 (6a′)^2 (1a″)^2 (2a″)^2 (7a′)^2 (8a′)^2 (9a′)^1/(3a″)^0 (valence electrons only).

Excitations originating from the SOMO (3b$_2$) into the virtual molecular orbitals 3b$_1$, 1a$_2$, 4b$_2$, and 4b$_1$ are interspaced between the excitations to the 3b$_2$ orbital. Again, the dipole-forbidden excitation 3b$_2$ → 3b$_1$ is computed lowest as predicted on qualitative arguments. The remaining transition to the 7a$_1$ was not obtained, because it corresponds to a higher root presently not computed. All have lower intensities, and the higher-energy state at 6.59 eV shows multireference character.

States resulting from double excitation are computed already around 4.5 eV, which is not surprising considering that several valence orbitals are close in energy. The first of these mixes with the 6a$_1$ → 3b$_1$ excitation giving rise to two states at 4.48 and 5.05 eV. If the double excitation is dominant in a given upper state, the *f* value to this state is relatively low, as expected for theoretical reasons.

3.3. Cyclic C$_5$H Isomer 3. The results calculated for the cyclic C$_5$H isomer **3** are collected in Table 4, and in Figure 4, the orbital energy diagram of its ground state is shown. Charge density contours of characteristic valence and low-lying virtual orbitals of C$_5$H isomer **3** are given in Figure 6.

The cyclic C$_5$H isomer **3** possesses a doublet X^{2}A′ ground state with the electron configuration ...(5a′)^2 (6a′)^2 (1a″)^2 (2a″)^2 (7a′)^2 (8a′)^2 (9a′)^1. The occupied molecular orbitals 8a′, 7a′, 2a″, and 6a′ can be expected to be the origin of single excitations to the half-filled 9a′ orbital (SOMO). Such transitions are calculated at 0.85, 1.67, 1.93, and 4.59 eV. Among these excitations, 3^{2}A′ ← X^{2}A′ (7a′ → 9a′) is the dominant transition. It is calculated with a *f* value of 0.06 and shows a contribution of 8a′ → 9a′ excitation, emphasizing the multireference character of this transition. Responsible for the relatively large oscillator

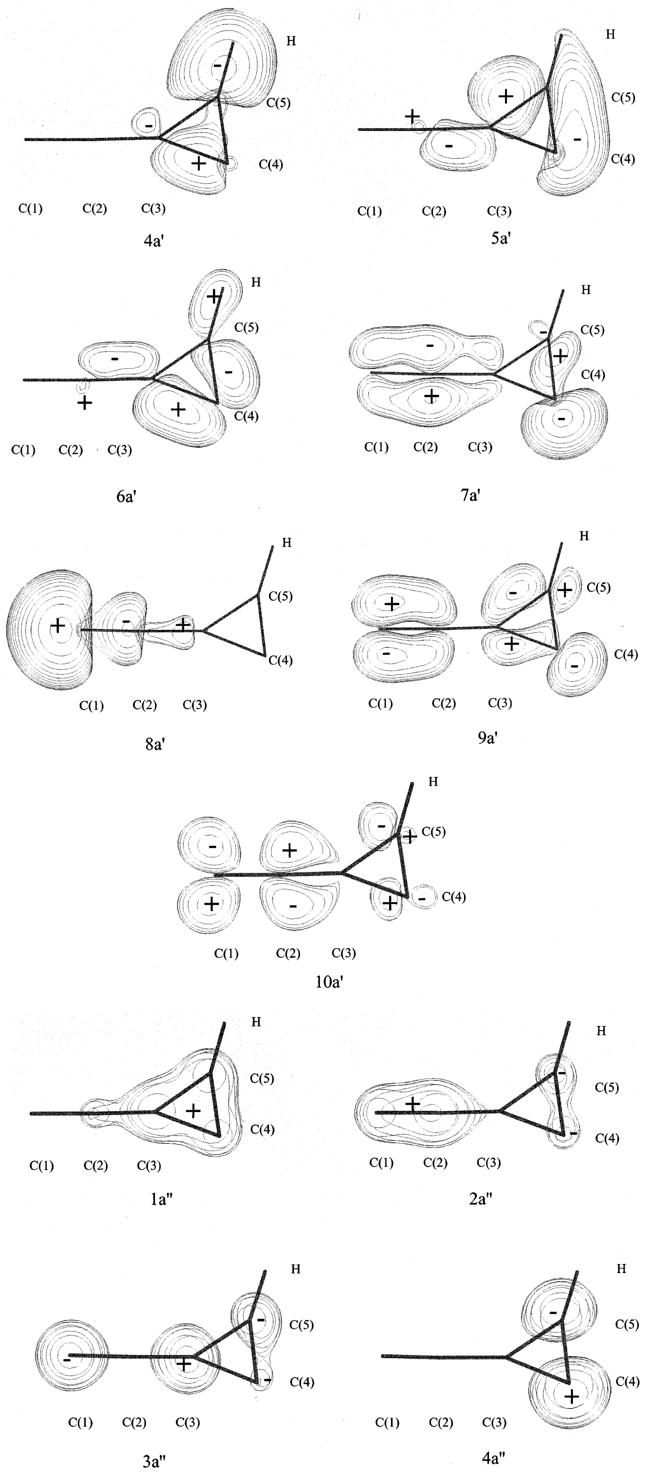

Figure 6. Charge density contours (molecular plane, contour value of 0.07) of characteristic valence and low-lying virtual (10a′, 3a″, 4a″) orbitals of the cyclic isomer **3** (Figure 1). The energetic ordering can be seen from Figure 4.

strength is the $\pi-\pi^*$[C(2)C(3)]-type 7a′ → 9a′ transition, whereas the 8a′ → 9a′ transition is of $\sigma-\pi^*$-type (Figure 6).

A number of excitations are found to populate the lowest unoccupied molecular orbital, 3a″ (LUMO). They originate from the valence MOs 9a′, 8a′, 2a″, and 7a′ and are computed at 2.53, 3.10, 3.89, and 3.98 eV. The analysis of reference configurations computed to be important for the $3^2A''$ state at 3.10 eV shows multireference character. The leading configuration results from 8a′ → 3a″ excitation, but a second configuration resulting from the excitation 7a′ 8a′ → 9a′ 3a″ is found to be important for this excited state. The corresponding linear combination ($4^2A''$) is calculated at 3.83 eV with a relatively large oscillator strength, which can be attributed to the $\sigma-\pi^*$-[C(3)C(4), C(3)C(5)] character of the 8a′ → 3a″ excitation as shown in Figure 6.

The single excitation 9a′ → 10a′ computed at 4.87 eV is also obtained with a sizable *f* value. This oscillator strength can be explained because the in-plane MO 9a′ is mainly of strong bonding π character for C(1)C(2) while the 10a′ MO on the contrary is a π^*-type for C(1)C(2) with a nodal plane between these two carbon centers.

At this point, a comparison of the two cyclic isomers of C_5H is appropriate. The shifting of the hydrogen from C(1) to C(5) in isomer **3** relative to isomer **2** changes mainly orbitals of a_1 and b_2 symmetry corresponding to a′ MOs in C_s symmetry, while the out-of-plain MOs b_1 and a_2 (a″ in C_s) are less affected by the in-plane σ(CH) bond. The SOMO 9a′ of isomer **3** is found to be slightly stabilized relative to the corresponding SOMO $3b_2$ of isomer **2**. The lone pair at C(1) in $3b_2$ transforms into a π-type bond between C(1) and C(2) in the corresponding MO of isomer **3**, while the remaining part of these MOs is unchanged. The HOMO $6a_1$ of isomer **2** forms a σ bond between C(4) and C(5). The corresponding 6a′ orbital of isomer **3** shows this bond to be strongly distorted. Additional bonding character at C(1)C(2), as well as C(2)C(3), causes a considerable stabilization of this MO compared to the $6a_1$ orbital. Thus in accordance with our calculations, the excitation $6a_1 \rightarrow 3b_2$ can be expected at lower transition energy compared to the 6a′ → 9a′ excitation. The HOMO 8a′ of isomer **3** primarily consists of a lone-pair at C(1). The corresponding $4a_1$ orbital of isomer **2**, which shows a σ-type C(1)H bond, is considerably lower in energy, so the excitation $4a_1 \rightarrow 3b_2$ corresponds to a root higher in energy presently not computed. The HOMOs of both isomers are calculated with about the same energy. Thus, the stabilization of the SOMO (9a′ compared to $3b_2$) is responsible for the smaller energy of the HOMO → SOMO transition. It is obtained at 1.27 and 0.85 eV for isomer **2** and isomer **3**, respectively.

The 7a′ MO of isomer **3** is of strong π-bonding character for C(1), C(2), and C(3) and shows a σ bond at C(4)C(5). The corresponding $2b_2$ orbital of isomer **2** consists mostly of a π-type bond at C(1)C(2) and is destabilized compared to 7a′. Therefore, the higher excitation energy computed for the $2b_2 \rightarrow 3b_2$ excitation (4.09 eV) compared to the 7a′ → 9a′ excitation (1.67 eV) is in line with our expectations. Obviously, $6a_1$ and $2b_2$ MOs of isomer **2** mix in the lower symmetry of isomer **3** and lead to the two MOs 6a′ and 7a′ in the C_s structure.

As can be seen from Figures 5 and 6, the orbitals $5a_1$ and 5a′ correspond to each other and show considerable deformations due to the lower C_s symmetry. The $1b_2$ level of isomer **2** shows bonding character at C(3)C(4) and C(3)C(5). A similar situation holds for the $1b_2$ and the 4a′ MO of isomer **3**. This 4a′ MO is stabilized by a σ bond at C(5)H and further bonding between C(3) and C(4). Therefore, the corresponding 4a′ → 9a′ transition energy is also expected to be larger compared to $1b_2 \rightarrow 3b_2$.

4. Summary and Conclusion

We performed multireference configuration interaction (MRD-CI) calculations for ground and excited states of three low-lying isomers of C_5H to predict approximate energies of characteristic transitions and oscillator strengths of the electronic spectra as a guideline for further experimental research. The spectrum of the linear isomer shows the first dipole-allowed transition around 2.5 eV ($^2\Delta \leftarrow X^2\Pi$) followed by five transitions in the region up to 4 eV. Relatively strong transitions are computed at about

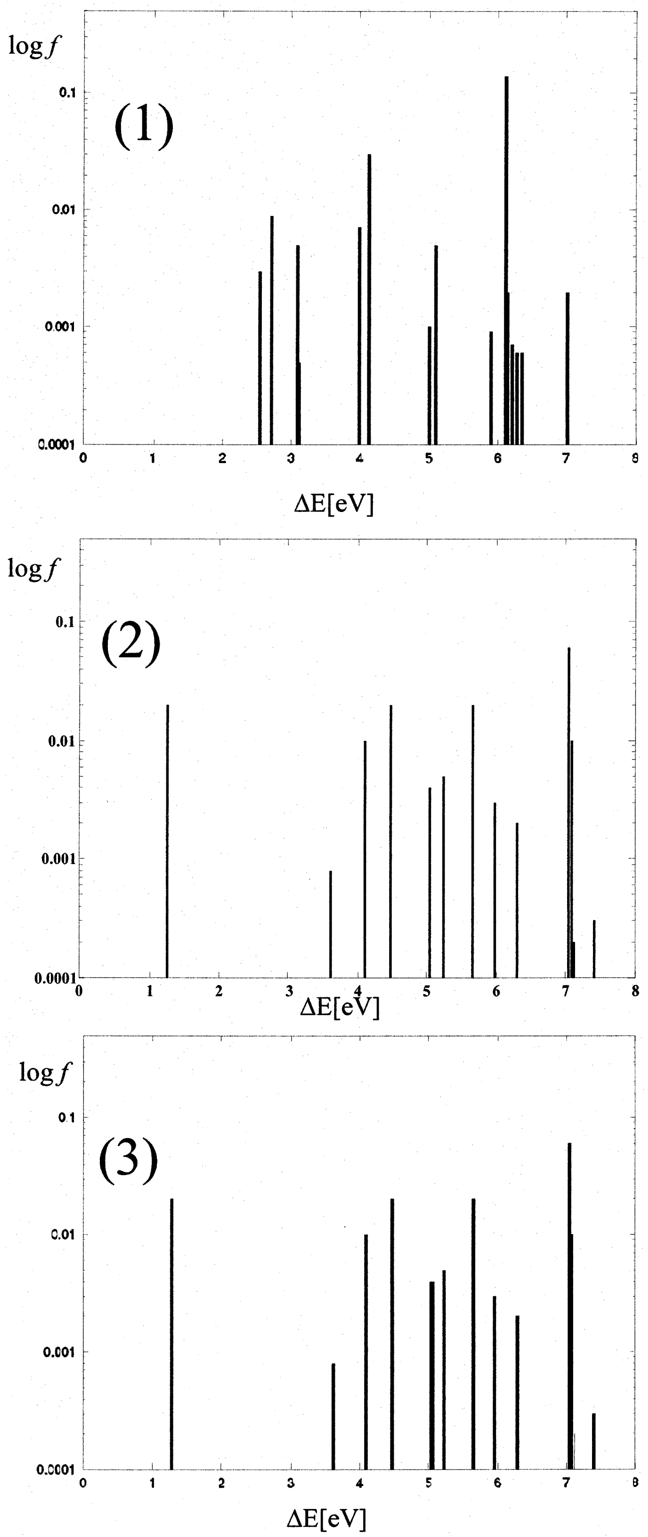

Figure 7. Graphical presentation of the calculated "stick" spectra of isomers **1**, **2**, and **3**. The corresponding numerical values can be seen from Tables 2, 3, and 4. The equilibrium structures of the isomers are given in Figure 1. Note the logarithmic scale for the *f* values.

4.1 eV ($^2\Pi \leftarrow X^2\Pi$) and 6.1 eV ($^2\Pi \leftarrow X^2\Pi$), which dominate the spectrum. The first dipole-allowed excitation of isomer **2** is computed around 1.3 eV ($^2A_1 \leftarrow X^2B_2$) and no further dipole-allowed excitations are obtained up to 3.6 eV ($^2A_2 \leftarrow X^2B_2$). For isomer **3**, five dipole-allowed excitations are computed in the energy interval between 0.8 eV ($^2A' \leftarrow X^2A'$) and 3.8 eV ($^2A'' \leftarrow X^2A'$), but only two of them with sizable intensity around 1.7 and 3.8 eV. Furthermore, two relatively strong ($f =$ 0.02−0.03) excitations are calculated around 4.6 and 4.9 eV. A comparison of the two cyclic isomers of C_5H is made, and the differences in the electronic spectra are consistent with the changes in the molecular orbitals of both isomers. A pictorial comparison of the spectra is shown in Figure 7. The vertical lines of intensity (in the logarithmic scale) correspond to vertical transitions with a Franck−Condon factor of unity, that is, a possible vibrational pattern is neglected in this representation. Nevertheless, it is clear that the best possibility to differentiate between the linear and cyclic isomers of C_5H by their electronic absorption spectra is the lower-energy window between 0.8 and 2.5 eV, because the cyclic isomers show transitions in this energy region, whereas the first strong transition of the linear isomer occurs at higher energies.

Acknowledgment. The present study is part of a Greek-German collaborative linkage grant "DAAD Program Griechenland IKYDIA 2001". The financial support from DAAD is gratefully acknowledged. We thank Michael Hanrath, this laboratory, for very helpful improvements in the DIESEL program package. Basis sets were obtained from the Extensible Computational Chemistry Environment Basis Set Database, version 11/29/01, as developed and distributed by the Molecular Science Computing Facility, Environmental and Molecular Sciences Laboratory, which is part of the Pacific Northwest Laboratory, P.O. Box 999, Richland, WA 99352, and funded by the U.S. Department of Energy.

References and Notes

(1) Weltner, W., Jr.; van Zee, R. *Chem. Rev.* **1989**, *89*, 1713.
(2) Van Orden, A.; Saykally, R. J. *Chem. Rev.* **1998**, *98*, 2313.
(3) Botschwina, P. *Theor. Chem. Acc.* **2000**, *104*, 160.
(4) Mühlhäuser, M.; Froudakis, G. E.; Peyerimhoff, S. D. *Chem. Phys. Lett.* **2000**, *324*, 195.
(5) Hanrath, M.; Peyerimhoff, S. D.; Grein, F. *Chem. Phys.* **1999**, *249*, 121.
(6) Mühlhäuser, M.; Froudakis, G. E.; Peyerimhoff, S. D. *Chem. Phys. Lett.* **2001**, *336*, 171.
(7) Mühlhäuser, M.; Froudakis, G. E.; Peyerimhoff, S. D. *Phys. Chem. Chem. Phys.* **2001**, *3*, 3913.
(8) Haubrich, J.; Mühlhäuser, M.; Peyerimhoff, S. D. *Phys. Chem. Chem. Phys.* **2002**, *4*, 2891.
(9) Hanrath, M.; Peyerimhoff, S. D. *Chem. Phys. Lett.* **2001**, *337*, 368.
(10) Cao, Z.; Peyerimhoff, S. D. *Phys. Chem. Chem. Phys.* **2001**, *3*, 1403.
(11) Maier, J. P. *Chem. Soc. Rev.* **1997**, 21.
(12) Schnell, M.; Mühlhäuser, M.; Froudakis, G. E.; Peyerimhoff, S. D. *Chem. Phys. Lett.* **2001**, *340*, 559.
(13) Giuffreda, M. G.; Deleuze, M. S.; Francois, J.-P. *J. Phys. Chem. A* **1999**, *103*, 5137.
(14) von Helden, G.; Gotts, N. G.; Palke, W. E.; Bowers, M. T. *Int. J. Mass Spectrom.* **1994**, *138*, 33.
(15) Maier, J. P. *J. Phys. Chem. A* **1998**, *102*, 3462.
(16) McCarthy, M. C.; Travers, M. J.; Kalmus, P.; Gottlieb, C. A.; Thaddeus, P. *Chem. Phys. Lett.* **1997**, *264*, 252.
(17) Freivogel, P.; Fulara, J.; Jakobi, M.; Forney, D.; Maier, J. P. *J. Chem. Phys.* **1995**, *103*, 54.
(18) Gottlieb, C. A.; Gottlieb, E. W.; Thaddeus, P. *Astron. Astrophys.* **1986**, *164*, L5.
(19) Cernicharo, M.; Kahane, C.; Gómez-Gonzáles, J.; Gúelin, M. *Astron. Astrophys.* **1986**, *164*, L1.
(20) Blanksby, S. J.; Dua, S.; Bowie, J. H. *J. Phys. Chem. A* **1999**, *103*, 5161.
(21) Crawford, T. D.; Stanton, J. F.; Saeh, J. C.; Schaefer, H. F., III *J. Am. Chem. Soc.* **1999**, *121*, 1902.
(22) Douglas, A. E. *Nature* **1977**, *269*, 130.
(23) Hanrath, M.; Engels, B. *Chem. Phys.* **1997**, *225*, 197.
(24) Buenker, R. J.; Peyerimhoff, S. D. *Theor. Chim. Acta* **1974**, *35*, 33; **1975**, *39*, 217.
(25) Poirier, R., Kari, R., Csizmadia, I., Eds. *Handbook of Gaussian Basis Sets*; Elsevier: Amsterdam, 1985; p 225 (Nr. 6.59.4).
(26) Dunning, T. H., Jr. *J. Chem. Phys.* **1989**, *90*, 1007.